Tetrahedron 69 (2013) 10361–10368

Contents lists available at ScienceDirect

Tetrahedron

journal homepage: www.elsevier.com/locate/tet

Size and branching effects on the fluorescence of benzylic dendrimers possessing one apigenin fluorophore at the core

Petr Vinš [a,b], Martina Vermachová [a], Pavel Drašar [a], Melisa del Barrio [c], Carmen Jarne [c], Vicente L. Cebolla [c,*], Abel de Cózar [b,d,e], Ronen Zangi [d,e], Fernando P. Cossío [b,d,*,†]

[a] Institute of Chemical Technology, Prague, Technická 5, 16628 Praha, Dejvice, Czech Republic
[b] Donostia International Physics Center (DIPC), P.O. Box 1072, 20018 San Sebastián – Donostia, Spain
[c] Instituto de Carboquímica, ICB-CSIC, P.O. Box 549, 50080 Zaragoza, Spain
[d] Department of Organic Chemistry I, Universidad del País Vasco – Euskal Herriko Unibertsitatea (UPV/EHU), P° Manuel de Lardizabal 3, 20018 San Sebastián – Donostia, Spain
[e] Ikerbasque, Basque Foundation for Science, E-48011 Bilbao, Spain

ARTICLE INFO

Article history:
Received 21 June 2013
Received in revised form 27 September 2013
Accepted 3 October 2013
Available online 10 October 2013

Keywords:
Dendrimers
Apigenin
Fluorescence
Photophysical properties
Quantum yield

ABSTRACT

Different generations of dendrimers incorporating one fluorescent core of apigenin and three Fréchet benzylic dendrons have been prepared. The chief geometric features of these dendrimers have been obtained by Molecular Dynamics simulations. These computational data suggest that the asphericities of dendrimers belonging to the third and fourth generations are considerably larger than those associated with lower radii of gyration. Fluorescence spectra of high generation dendrimers evolve along time and quantum yields show an appreciable lowering for the fourth generation dendrimer. All these data suggest aggregation phenomena and lower quantum yields for nonspheric dendrimers in solution.

1. Introduction

Since the discovery in 1978 of 'cascade molecules' by Vögtle et al.,[1] dendrimers (as termed by Tomalia[2]) have emerged as a very important class of macromolecules with well-defined architectures. The nature of the cores, the different spacers, and end groups, as well as the degrees of branching can be chosen among many different building blocks,[3] thus giving rise to a plethora of different families of dendrimers[4] with many applications in, among other fields, catalysis,[5] materials science,[6] supramolecular chemistry,[7] and biomedicine.[8]

The structure and shape of dendrimers are difficult to determine and actually the usual analytical techniques[9] are pushed to their limits to characterize the identity, purity, and structural elucidation of these macromolecules. In this respect, computational methods are very useful to describe adequately both the geometrical and dynamic behavior of dendritic molecules.[10] Pioneering studies proposed that dendrimers in general exhibit density profiles in which a global minimum is located at the center, with a monotonic increase towards the periphery.[11] However, this general model was refined[12] and now it is generally admitted that this density profile is more complex, thus resulting in dense core regions and relatively less dense peripheries.

Fluorescent dendrimers[13] are particularly interesting because of their potential as analytical tools[14] or in light-harvesting devices,[15] organic light emitting diodes[16] (OLEDs), solar cells[6a] or displays.[17] The chosen fluorophores can be installed at different parts of the macromolecule. In most cases, diverse fluorophores and/or donor/acceptor systems can be incorporated within the different branches or at the periphery. In these cases, however, the structure optical response relationship is difficult to rationalize. In previous work on dendrimers carried out in our group, we have analyzed the catalytic activity of dendrimers with one active site at the core. In this case a rationale of the catalytic activity of different dendrimers possessing Fréchet dendrons was developed.[18] Following this approach, in this paper we would like to present a simple model describing the structure activity quantitative relationship of fluorescent dendrimers incorporating only one fluorophore at the core. As a case study, we have chosen apigenin,[19] a weak blue light emitting fluorophore that possesses three phenol groups amenable to Williamson coupling reactions with different Fréchet dendron bromides. The interplay between the 4*H*-

* Corresponding authors. E-mail address: fp.cossio@ehu.es (F.P. Cossío).
† Fax: +34 943 015270.

0040-4020/$ – see front matter © 2013 Elsevier Ltd. All rights reserved.
http://dx.doi.org/10.1016/j.tet.2013.10.002

chromen-4-one fluorophore and the phenyl chromophores of the branches and at the periphery should result in different photophysical responses for the successive generations of dendrimers. As we will see, this design has permitted to find a simple model that connects the quantum yield of the fluorescent emission with an easy to compute and intuitive combined geometrical parameter.

2. Results and discussion

2.1. Preparation of apigenin derivatives

We prepared compounds **3a**–**f** by Williamson reaction between **1** and halides **2a**–**f** in the presence of different bases (Scheme 1).

The reaction conditions reflect the increasing difficulty to accomplish the formation of the three C–O bonds along the different dendritic generations. Thus, formation of small compounds **3a**–**c** (Apigenin derivatives **3b**, **c** being the zeroth and first generation **G0** and **G1** in the dendrimer series) required NaH as a base and 20 h at room temperature. In the case of dendrimers **3d**–**f**, Williamson couplings involving Fréchet dendrons **2d**–**f** required potassium carbonate, 18-crown-6 as a cryptand of potassium and heating at 80 °C.

2.2. Molecular simulations and structural parameters of dendrimers 3b–f

In order to gain a better understanding of the structural properties of compounds **3b**–**f** and their relationship with the observed properties (vide infra), we performed atomistic molecular dynamics (MD) simulations on these compounds using the MM3 force field.[20] Evolution of dendrimers **3b**–**f** (**G0**–**G4**) was simulated along 1000 ps.

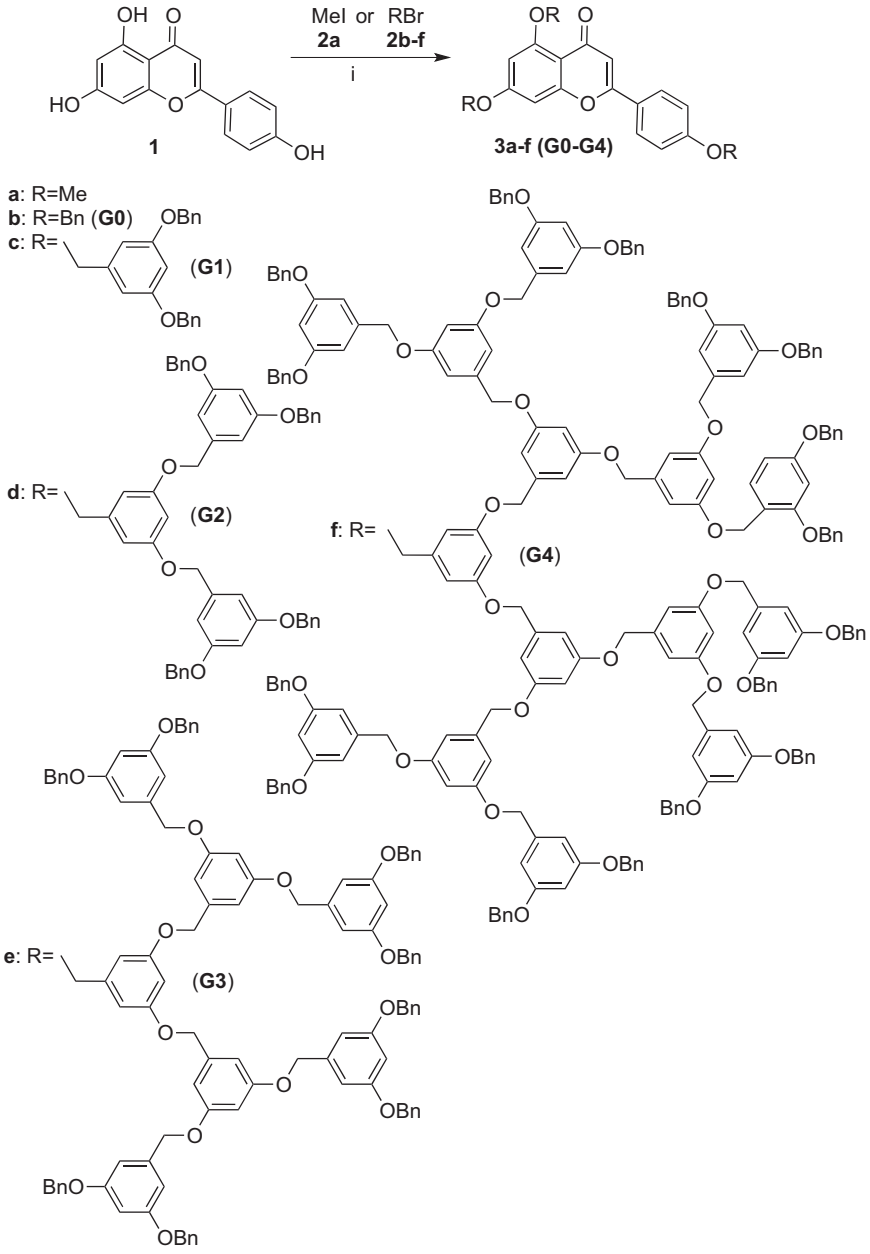

Scheme 1. Synthesis of ethers **3a**–**f** (**G0**–**G4**) from apigenin **1**. Reagents and conditions: *i*: NaH (for **G0**, **G1**) or K_2CO_3 (for **G2**–**G4**), 18-crown-6 (for **G2**–**G4**), rt (for **G0**, **G1**) or 80 °C (for **G2**–**G4**). Bn=Benzyl.

The chemical yields of purified products were relatively low (15–40%, see Experimental section) but satisfactory enough for our purposes.

During the production time of the MD simulations, the fluctuating energy values were observed to be stable within the thermal limits (the relative root mean squared fluctuation in the energy ranged from 0.01 for the smallest system to 0.001 for the largest system), as it can be seen by inspection of the energy profiles gathered in Fig. 1.

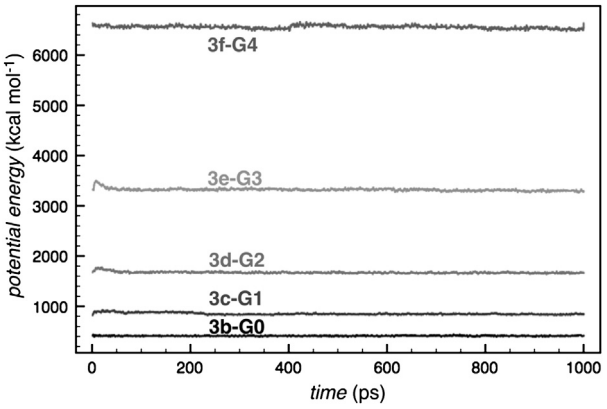

Fig. 1. MM3 potential energy profiles for dendrimers **3b**–**f** (**G0**–**G4**) along the MD simulations.

The general shape of compounds **3b**-**G0** and dendrimers **3c**–**f** (**G1**–**G4**) can be appreciated in Fig. 2, in which we have superimposed the 10 most stable geometries obtained during the production time of the respective MD simulations. From these data it can be readily seen that lower dendrimers **3b**-**G0**, **3c**-**G1** and **3d**-**G2** permit contacts between the apigenin and the external medium, whereas in higher dendrimers **3e**-**G3** and **3f**-**G4** these contacts are much more difficult.

In order to quantify these geometric differences, we computed the radii of gyration for all the points generated along the MD simulations. The radius of gyration R_g is given by the following expression:

$$R_g = \left[\frac{\sum_{i=1}^{n} m_i(\vec{r}_i - \vec{g})(\vec{r}_i - \vec{g})}{\sum_{i=1}^{n} m_i}\right]^{1/2} \quad (1)$$

where m_i is the mass of atom i (i=1,2,…,n), $\vec{r}_i$ is its position vector, and $\vec{g}$ is the position vector of the center of masses:

$$\vec{g} = \frac{\sum_{i=1}^{n} m_i \vec{r}_i}{\sum_{i=1}^{n} m_i} \quad (2)$$

The fluctuation of the R_g values along the MD simulations for the different generations **G0**–**G4** are gathered in Fig. 3 and the average values are reported in Table 1. Our results indicate that the R_g values of **3b**-**G0** and **3c**-**G1** are similar during most of the production time. The values obtained for **3d**-**G2** are slightly higher. Dendrimers **3e**-**G3** and **3f**-**G4** exhibit consistently larger radii of gyration and lower fluctuations, which indicate more rigid structures and larger atom densities at the respective cores and peripheries.

The square of R_g is equal to the trace of the gyration tensor S of a given molecule and it is defined by Eq. 3:

$$S = \frac{1}{M}\begin{pmatrix} \sum_i m_i(x_i - x_{cm})(x_i - x_{cm}) & \sum_i m_i(x_i - x_{cm})(y_i - y_{cm}) & \sum_i m_i(x_i - x_{cm})(z_i - z_{cm}) \\ \sum_i m_i(y_i - y_{cm})(x_i - x_{cm}) & \sum_i m_i(y_i - y_{cm})(y_i - y_{cm}) & \sum_i m_i(y_i - y_{cm})(z_i - z_{cm}) \\ \sum_i m_i(z_i - z_{cm})(x_i - x_{cm}) & \sum_i m_i(z_i - z_{cm})(y_i - y_{cm}) & \sum_i m_i(z_i - z_{cm})(z_i - z_{cm}) \end{pmatrix} \quad (3)$$

$$\mathrm{tr}(S) = R_g^2 = \mathrm{tr}\begin{pmatrix} L_1^2 & 0 & 0 \\ 0 & L_2^2 & 0 \\ 0 & 0 & L_3^2 \end{pmatrix} \quad (4)$$

In Eq. 3 M stands for the total mass of the dendrimer. In the last term of Eq. 4 the tensor S is diagonalized such that the components L_i (i=1,2,3) of R_g with respect to the corresponding main axes are assigned according to the following criterion:

$$L_1^2 > L_2^2 > L_3^2 \quad (5)$$

These L_i values can be used to quantify the shape of the molecule being considered. Thus, the asphericity a_s of one given molecular geometry is defined as[21]

$$a_s = L_1^2 - \frac{1}{2}\left(L_2^2 + L_3^2\right) \quad (6)$$

According to Eq. 6, a_s reflects the anisotropy of the molecule with respect to the principal axes. For a perfect sphere, the magnitudes of the three main radii are identical (L_1=L_2=L_3) and therefore a_s=0. In our case, values of a_s>0 reflect the increasing anisotropy of dendrimers **3b**–**f** by departure from perfect sphericity. The average values of L_i and a_s are gathered in Table 1.

Our computed values for asphericity show closely related values for **G0** and **G2**. First generation dendrimer **G1** is more spheric than apigenin derivatives **G0** and **G2**, **G3** showing a somewhat larger value of about 64 Å^2. However, the largest asphericity value was computed for **G4**, with a value of a_s almost twice than that obtained for **G3** (See Fig. 4 and Table 1). This suggests that the hydrodynamic behavior of **G4** is determined by a larger departure from sphericity and aggregation phenomena to form more isotropic structures with lower a_s values should be expected.[22]

2.3. Photophysics of compounds 3a–f

Absorption spectra of compounds **3a**–**f** show two zones, which provide different structural information (Fig. 5). One of them, associated with a maximum near 315 nm, is related to the fluorophore core. The other zone, with a maximum absorption near 280 nm, may provide some information on the fluorescence generated by the benzylic dendrons. In all cases, we observed that absorbances at both 280 and 315 nm increase linearly with concentration. Inspection of Fig. 5 shows quite similar UV spectra for **G0**–**G2**, with a distinctive profile for **G4**, **G3** being between both subsets. This can be explained in terms of an effect of the medium. According to Toptygin[23] the extinction coefficient as well as the radiative decay rate depend on the refractive index. In spite of the fact that the increase with the refractive index is higher for the radiative decay rate, it also occurs for the extinction coefficient and it was observed for the first generations of dendrimers.

Quantum yields were measured at the previously described two excitation wavelengths. Apigenin exhibits double fluorescent emission in methanol, with two maxima at 430 nm and 534 nm.[24] When excitation is done at 300 nm, emission shows a maximum at 430, and a shoulder at 534 nm. By exciting at 357 nm, only emission at 534 nm is obtained. The emission spectra of the dendrimers when exciting at 280 nm are similar than those when exciting at 315 nm (see Supplementary data for further information). This has

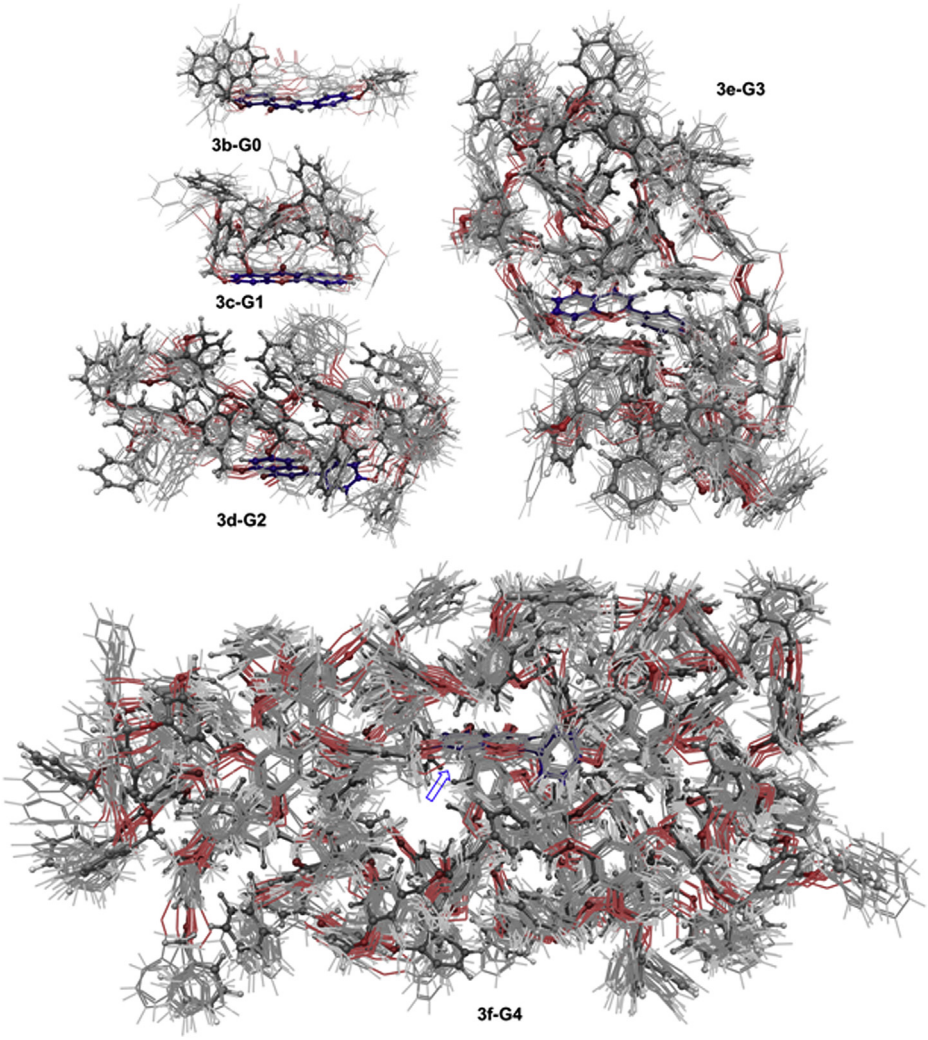

Fig. 2. Snapshots from the MD simulations of dendrimers **3b-G0**, **3c-G1**, **3d-G2**, **3e-G3** and **3f-G4**. The apigenin core in each dendrimer is highlighted in blue. The most stable structures are gathered in ball & stick representation. The remaining structures correspond to the 10 most stable structures within the 1000 ps simulation time. The hollow arrow in **3f-G4** indicates the position of the apigenin core.

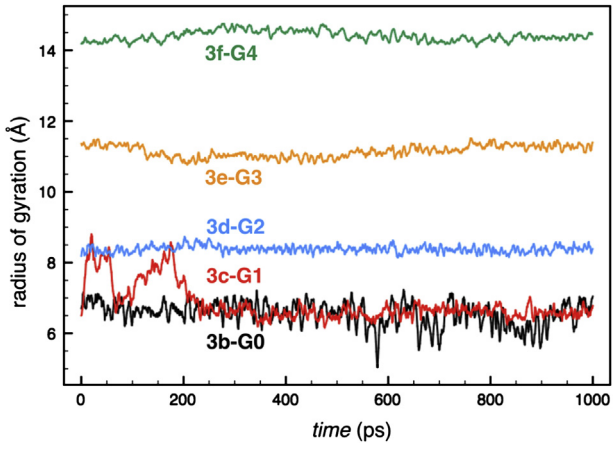

Fig. 3. Evolution of the radius of gyration of dendrimers **3b**–**f** (**G0**–**G4**) along the production time of MD simulations.

been reported[25] to be due to an intramolecular proton transfer between a phenolic OH (in C-5) and the oxygen of carbonyl (in C-4). In the case of **3a**, the latter emission is not present since the phenolic OH has been methoxylated and, therefore, there is no possibility for an intramolecular proton transfer. As a consequence, the quantum yield of **3a** (1.7×10^{-3}, see Table 2) is higher than that of apigenin (4×10^{-4}).

Table 1
Average values[a] of radius of gyration ($\langle R_g\rangle$, in Å), its components along the main axes L_1–L_3 (in Å) and asphericities ($\langle a_s\rangle$, in Å^2) of dendrimers **3b**–**f** (**G0**–**G4**)

Dendrimer	$\langle R_g\rangle$	$\langle L_1\rangle$	$\langle L_2\rangle$	$\langle L_3\rangle$	$\langle a_s\rangle$
3b-G0	6.07±0.07	5.59±0.26	2.07±0.05	1.20±0.15	28.30±1.42
3c-G1	6.53±0.02	5.05±0.79	3.52±0.06	2.23±0.10	16.84±1.07
3d-G2	8.36±0.01	6.75±0.10	4.20±0.10	2.74±0.78	32.94±0.34
3e-G3	11.21±0.12	9.15±0.17	5.16±0.10	3.66±0.05	63.73±0.50
3f-G4	14.82±0.16	12.29±0.46	6.85±0.40	4.83±0.08	116.05±1.23

[a] All values correspond to the average values obtained along the MD simulations using the MM3 force field and Eqs. 1–5.

Quantum yields and radiative constants k_r of dendrimers were found to be higher than those of **3a**, and increase on going from **3b-G0** to **3d-G2** at λ_{exc}=315 nm. However, from this latter dendrimer these values decrease to achieve a quantum yield of **3f-G4** at 280 nm similar to that of **3a**. In the case of λ_{exc}=280 nm, **3c-G1** showed the highest quantum yield and a monotonous decrease was observed on going from **G2** to **G4**. The observed enhancements of fluorescence can be related to the contribution of the refractive index, according to the Toptygin equation:[23]

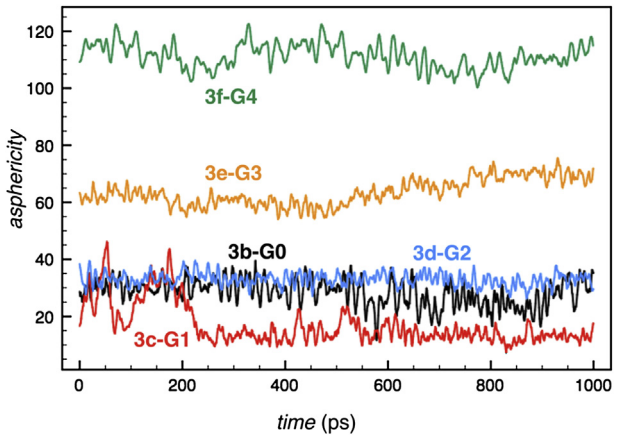

Fig. 4. Evolution of the asphericity of dendrimers **3b**–**f** (**G0**–**G4**) along the production time of MD simulations.

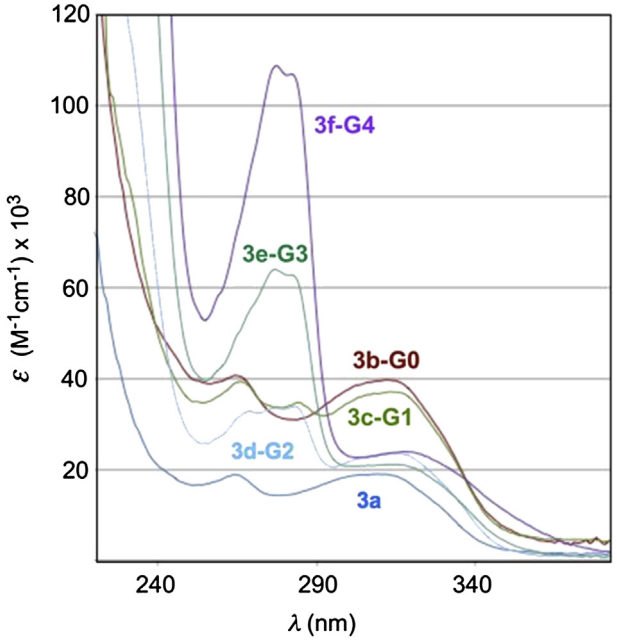

Fig. 5. Absorption spectra of compounds **3a**–**f** in THF.

Table 2
Photophysical data of apigenin derivatives **3a**–**f**

Dendrimer	Φ^a (315 nm)	Φ^a (280 nm)	τ (ns)[b]	$k_r\times10^{-9}$ (s^{-1})[c]	$k_{nr}\times10^{-9}$ (s^{-1})[d]
3a	0.0017	0.0018	0.88	0.001924	1.129810
3b-G0	0.0053	0.0045	0.82	0.006498	1.219443
3c-G1	0.0095	0.0055	0.86	0.011017	1.148672
3d-G2	0.0112	0.0039	0.86	0.012984	1.146302
3e-G3	0.0033	0.0021	1.03	0.003219	0.972390
3f-G4	0.0077	0.0017	0.75	0.010216	1.316572

[a] Quantum yields measured in THF at different excitation wavelengths using quinine sulfate as standard (See Experimental section).
[b] Time-domain excited-state lifetime.
[c] Radiative constants.
[d] Non-radiative constants, measured in THF.

$$k_r = nf^2k_{r0} \tag{7}$$

where n is the refractive index of the host medium; f is a function of n, and depends on the geometry of the local environment, and k_{r0} is the radiative decay constant in vacuum. In the case of **3a**, n is that of solvent. In the case of dendrimers **G0**–**G4**, the n value associated with the local medium that would correspond to that of the aromatic dendrons in the microenvironment of the fluorophore. It is reasonable to think that, at least for dendrimers **G0**–**G2**, it will be higher than that of the solvent. Likewise, it should become higher with the degree of branching. However, our results also suggest that from a certain degree of branching on, aggregations of dendrimers occur in THF. This should lead to a decrease of the fluorescent emission, as it can be seen by inspection of the quantum yields reported in Table 2.

Emission spectra of higher dendrimers were found to evolve over time, which also suggests aggregation phenomena. Fig. 6 shows the spectra of solutions of different concentrations of **3e**-**G3** 48 h after their preparation, showing that these spectra and the corresponding aggregates become stable after sufficient time. These data are consistent with the structural results obtained from the MD simulations: the lower asphericity shown by **G3** is, at least in part, responsible for these aggregation phenomena and, into a higher extension, those associated with **G4**.

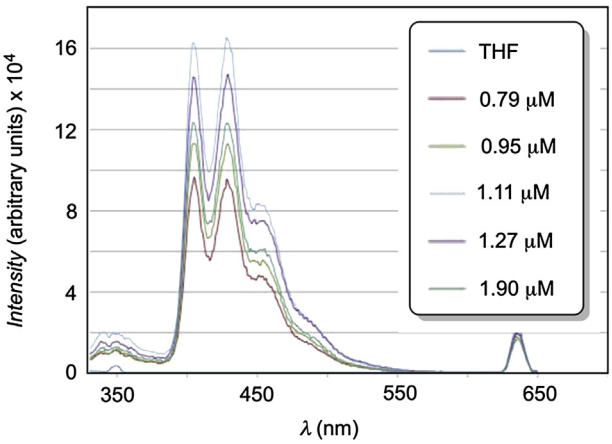

Fig. 6. Emission spectra of **3e**-**G3** at five different concentrations and after 48 h of their preparation.

From the data collected in Tables 1 and 2, the evolution of the quantum yields along the **G1**–**G4** series can be quantified. We have found a linear correlation between the $\langle R_g\rangle/\langle a_s\rangle$ ratio and the quantum yield associated with the fluorescent emission with a wavelength of 280 nm, namely that associated with $\pi\rightarrow\pi^*$ transitions involving the Fréchet dendrons of **G1**–**G4**. This correlation is given by the following expression:

$$\Phi = K_G\frac{\langle R_g\rangle}{\langle a_s\rangle} \tag{8}$$

with K_G=0.014 Å (Fig. 7). Our attempts to find a similar correlation associated with the excitation of the apigenin fluorophore met with no success. These results suggest that the combined $\langle R_g\rangle/\langle a_s\rangle$ parameter can be useful to design dendrimers with better photophysical properties by increasing the generation number (with larger radii of gyration) while keeping asphericities as low as possible. Note however that the relation in Eq. 8 is found to hold for dendrimers with shapes studied in this work, which are characterized by relatively large value of asphericity. Further studies are needed in order to elucidate the behavior of dendrimers with smaller value of $\langle a_s\rangle$ and, in particular, for perfectly spherical molecules ($\langle a_s\rangle$) because then the right hand side of Eq. 8 diverges.

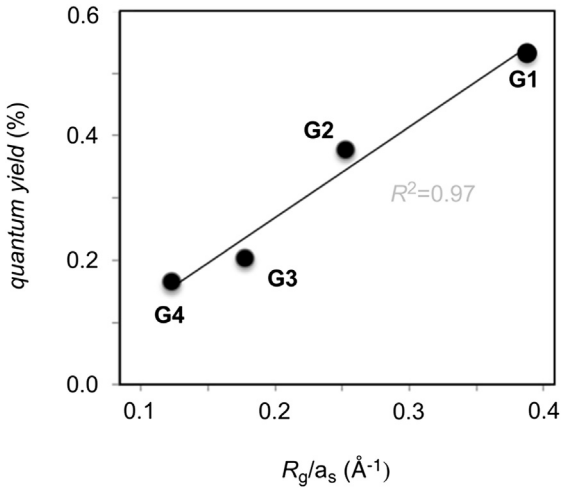

Fig. 7. Correlation between structural data of dendrimers **G1**–**G4** and quantum yields measured with an excitation wavelength of 280 nm.

3. Conclusions

In this paper we report the preparation and the main geometrical and photophysical properties of different dendrimers possessing an apigenin fluorophore at the core and different Fréchet dendrons. The coupling between the core and the dendrons has been carried out via Williamson reactions between the three phenolic groups of apigenin and the corresponding Fréchet bromides. A transition from nearly spherical to highly aspherical dendrimers has been detected on going from the first three generations to **G3** and, specially, **G4**. It is found that for lower generation dendrimers the quantum yields of the fluorescent emissions increase with the generation number or the radius of gyration as it could be expected for more isolated fluorophores. This maximum quantum yield is achieved for **G2**. However, there is a significant decay in the quantum yields of **G3** and **G4**, which parallels an increase in asphericity for these latter dendrimers. These data, together with the evolution of the emission spectra, indicate that aggregation phenomena are relevant in **G3** and **G4**, thus resulting in more efficient nonradiative decays and therefore in lower quantum yields. These results suggest that, in order to improve the quantum yields of fluorescent emission of dendrimers highly spheric low associative dendrimers should be designed.

4. Experimental section

4.1. Computational methods

All the computational studies reported in this paper were based upon molecular mechanics[26] (MM) and molecular dynamics (MD).[27] In both, the MM3 method developed by Allinger et al. as implement in the *MacroModel*[28] package was used. All MD simulations were performed with SHAKE[29] to constrain the C–H bonds. The temperature was set up to 298 K. The system was equilibrated for 1 ns with time steps of 1 fs. This equilibration time is 10 times longer than the expected value for the relaxation time of dendrimers[30] of this size. The production run was started from this point and lasted another nanosecond with time steps of 1 fs. In all cases, we observed that during the production period, the energy and temperature of the whole system were equilibrated. During the production run, the coordinates were saved each picosecond, which implies a total of 1000 structures. These structures were used to calculate the averages of the properties specified below. To calculate these properties, programs based on the DYNAMO library[31] were written.

4.2. General experimental methods

Reagents and solvents were purchased from commercial suppliers and used without further purification. Fréchet-type dendrons of generation number one to four **2c**–**f** were prepared according to procedure reported by Fréchet.[32] NaH was used in form of 60% (w/w) dispersion in mineral oil. Column chromatographies were carried out with silica gel 60 (0.040–0.063 mm). All melting points are uncorrected. NMR spectra were recorded in $CDCl_3$ and using frequencies as indicated bellow. Mass spectra were measured using electrospray ionization at positive mode. MALDI-TOF MS spectra were measured using trihydroxyacetophenone in 60% acetonitrile with 0.1% of TFA as matrix. MALDI-TOF spectrum of dendrimer **3f** was recorded in linear mode using sinapic acid in 60% acetonitrile with 0.1% of TFA as matrix.

4.2.1. 5,7,4′-Trimethoxyflavone,[33] ***3a***. To a solution of apigenin (50 mg, 0.19 mmol) in dry dimethylformamide (2 ml) was added NaH (20 mg, 0.5 mmol), under cooling by ice bath. After stirring for 10 min under argon, methyl iodide (0.15 ml, 2.56 mmol) was added dropwise. The reaction mixture was stirred for 20 h at room temperature and then, it was diluted by dichloromethane, washed by water, organic phases collected and dried ($MgSO_4$), and evaporated under reduced pressure. The residue was purified by flash chromatography on silica gel (CH_2Cl_2/MeOH) and by precipitation by hexanes from ethyl acetate to yield title product as yellow solid (40%, 30 mg): IR 1640, 1601, 1573, 1511 cm^{-1}; ^{1}H NMR (300 MHz, $CDCl_3$, 25 °C) δ=7.81 (d, J=8.5 Hz, 2H), 6.98 (d, J=8.5 Hz, 2H), 6.59 (s, 1H), 6.54 (d, J=1.8 Hz, 1H), 6.35 (d, J=2.3 Hz, 1H), 3.94 (s, 3H), 3.90 (s, 3H), 3.87 (s, 3H) ppm; ^{13}C NMR (126 MHz, $CDCl_3$, 25 °C) δ=177.60, 163.88, 162.02, 160.89, 160.65, 159.82, 127.58 (2C), 123.85, 114.33 (2C), 109.23, 107.69, 96.06, 92.81, 56.40, 55.71, 55.45 ppm. MS (ESI) m/z: found 312.9 [M+H]$^+$; calcd 313.1.

4.2.2. 4′,5,7-Trisbenzyloxyflavone,[34] ***3b-G0***. To a solution of apigenin (40 mg, 0.15 mmol) in dry dimethylformamide (2 ml) was added NaH (20 mg, 0.5 mmol), under cooling by ice bath. After stirring for 10 min under argon, benzyl bromide (0.2 ml, 1.69 mmol) was added dropwise. The reaction mixture was stirred for 20 h at room temperature and then, it was diluted by ethyl acetate, washed by water, organic phases collected and dried ($MgSO_4$), and evaporated under reduced pressure. The residue was purified by flash chromatography on silica gel (gradient of ethyl acetate in toluene/hexane (60/40 v/v)) and precipitated by hexanes from ethyl acetate to yield title product (25%, 21 mg) as slightly yellow solid: IR 1638, 1601, 1509, 1163 cm^{-1}; ^{1}H NMR (300 MHz, $CDCl_3$, 25 °C) δ=7.82 (d, J=8.5 Hz, 2H), 7.62 (d, J=7.6 Hz, 2H), 7.28–7.49 (m, 13H), 7.07 (d, J=8.5 Hz, 2H), 6.64 (d, J=2.1 Hz, 1H), 6.58 (s, 1H), 6.49 (d, J=1.8 Hz, 1H), 5.23 (s, 2H), 5.14 (s, 2H), 5.11 (s, 2H) ppm; ^{13}C NMR (126 MHz, $CDCl_3$, 25 °C) δ=177.32, 162.81, 161.17, 160.65, 160.54, 159.70, 136.44, 136.29, 135.73, 128.75, 128.74, 128.69, 128.55, 128.41, 128.21, 127.64, 127.59, 127.45, 126.58, 124.13, 115.23, 109.87, 107.82, 98.37, 94.28, 70.77, 70.47, 70.17 ppm. MS (ESI) m/z: found 541.5 [M+H$^+$]; calcd 541.6.

4.2.3. Dendrimer ***3c-G1***. To a solution of apigenin (19 mg, 0.070 mmol) in dry dimethylformamide (2 ml) was added NaH (15 mg, 0.38 mmol), under cooling by ice bath. The mixture was stirred for 10 min under argon and then, **2c** (150 mg, 0.39 mmol) was added. The reaction mixture was stirred for 20 h at room temperature and then it was diluted by dichloromethane and washed by water. Organic phases were collected, dried ($MgSO_4$), and evaporated under reduced pressure. The residue was purified by flash chromatography on silica gel (gradient of ethyl acetate in toluene/hexane (60/40 v/v)) and precipitated two times by pentane from ethyl acetate to yield corresponding product (25%, 21 mg) as

a colorless solid: mp 113–114 °C, IR 1640, 1592, 1145, 1049 cm^{-1}; ^1H NMR (500 MHz, $CDCl_3$, 25 °C) δ=7.81 (d, J=8.8 Hz, 2H), 7.28–7.47 (m, 30H), 7.04 (d, J=9.1 Hz, 2H), 6.93 (d, J=2.3 Hz, 2H), 6.65–6.71 (m, 4H), 6.62 (s, 1H), 6.52–6.62 (m, 4H), 6.45 (d, J=2.1 Hz, 1H), 5.18 (s, 2H), 5.08 (s, 6H), 5.04 (s, 10H) ppm; ^{13}C NMR (126 MHz, $CDCl_3$, 25 °C) δ=177.24, 162.63, 161.04, 160.56, 160.28, 160.25, 160.21, 159.64, 159.53, 139.01, 138.75, 138.13, 136.98, 136.69, 136.63, 128.59, 128.47, 128.05, 128.03, 127.84, 127.67, 127.63, 127.51, 127.50, 124.19, 115.25, 109.90, 107.84, 106.41, 106.32, 105.31, 101.81, 101.68, 101.61, 98.32, 94.37, 70.60, 70.26, 70.17, 70.15, 70.10, 70.02 ppm. MS (ESI) m/z found 1176.8 $[M+H^+]$, calcd 1176.44; Anal. Calcd for $C_{78}H_{64}O_{11}$: C, 79.57, H, 5.48. Found: C, 79.78, H, 5.64.

*4.2.4. Dendrimer **3d**-**G2**.* Apigenin (7.4 mg, 0.027 mmol) was dissolved in mixture of DMF and toluene (2 ml, 1/1 v/v). Then, K_2CO_3 (75 mg, 0.54 mmol), 18-crown-6 (5 mg, 0.02 mmol) and **2d** (154 mg, 0.19 mmol) were added. The reaction mixture was stirred at 80 °C for 20 h. Then, it was diluted by dichloromethane and washed by water. Organic phases were collected, dried ($MgSO_4$), and evaporated under reduced pressure. The residue was purified by flash chromatography on silica gel (gradient of diethyl ether in toluene/hexane (75/25 v/v)) and precipitated by pentane from THF to yield title product (40%, 28 mg) as a colorless solid glass: IR 1641, 1592, 1145, 1044 cm^{-1}; ^1H NMR (500 MHz, $CDCl_3$, 25 °C) δ=7.73 (d, J=9.1 Hz, 2H), 7.27–7.47 (m, 60H), 7.00 (d, J=9.1 Hz, 2H), 6.93 (d, J=2.1 Hz, 2H), 6.62–6.74 (m, 15H), 6.43–6.61 (m, 12H), 6.47 (d, J=2 Hz, 1H), 5.15 (s, 2H), 4.90–5.07 (m, 40H) ppm; ^{13}C NMR (126 MHz, $CDCl_3$, 25 °C) δ=177.18, 162.65, 161.01, 160.54, 160.18, 160.14, 160.08, 159.63, 159.52, 143.15, 139.47, 139.15, 139.07, 139.00, 138.74, 138.11, 136.85, 136.73, 136.72, 128.57, 128.51, 128.00, 127.99, 127.90, 127.61, 127.54, 127.51, 127.29, 124.14, 115.18, 109.86, 107.82, 106.47, 106.41, 106.39, 105.28, 101.83, 101.70, 101.59, 101.56, 70.12, 70.07, 70.01, 70.00 ppm. MS (MALDI-TOF) m/z found 2448.5 $[M+H]^+$, calcd 2449.9; found 2472.4 $[M+Na]^+$, calcd 2471.9; found 2488.5 $[M+K]^+$, calcd 2487.9; Anal. Calcd for $C_{162}H_{136}O_{23}$: C, 79.39, H, 5.59. Found: C, 79.22, H, 5.47.

*4.2.5. Dendrimer **3e**-**G3**.* Apigenin (6.1 mg, 0.023 mmol) was dissolved in mixture of DMF and toluene (2 ml, 1/1 v/v). Then, K_2CO_3 (30 mg, 0.22 mmol), 18-crown-6 (5 mg, 0.019 mmol) and **2e** (150 mg, 0.091 mmol) were added. The reaction mixture was stirred at 80 °C for 20 h. Then, it was diluted by dichloromethane and washed by water. Organic phases were collected, dried ($MgSO_4$), and evaporated under reduced pressure. The residue was purified by flash chromatography on silica gel (gradient of diethyl ether in toluene/hexane (75/25 v/v)) and precipitated two times by pentane from THF to yield title product (25%, 34 mg) as colorless solid glass: IR: 1641, 1592, 1147, 1044 cm^{-1}; ^1H NMR (500 MHz, $CDCl_3$, 25 °C) δ=7.67 (d, J=8.8 Hz, 2H), 7.18–7.47 (m, 120H), 6.93 (m, 4H), 6.45–6.72 (m, 63H), 6.41 (br s., 1H), 5.09 (br s., 2H), 4.78–5.04 (m, 88H) ppm; ^{13}C NMR (126 MHz, $CDCl_3$, 25 °C) δ=160.14, 160.12, 160.08, 160.06, 160.04, 159.96, 139.48, 139.28, 139.17, 136.79, 136.74, 128.55, 128.54, 128.51, 127.96, 127.93, 127.91, 127.52, 127.51, 106.42, 106.36, 101.70, 101.63, 101.57, 101.54, 70.10, 70.06, 70.03, 69.96, 69.93 ppm. MS (MALDI-TOF) m/z found 4996.4 $[M+H]^+$, calcd 4995.9; found 5019.5 $[M+Na]^+$, calcd 5018.0. Anal. Calcd for $C_{330}H_{280}O_{47}$: C, 79.31, H, 5.65. Found: C, 79.46, H, 5.78.

*4.2.6. Dendrimer **3f**-**G4**.* Apigenin (1.6 mg, 0.0059 mmol) was dissolved in mixture of DMF and toluene (1 ml, 1/1 v/v). Then, K_2CO_3 (15 mg, 0.11 mmol), 18-crown-6 (3 mg, 0.011 mmol) and **2f** (70 mg, 0.0208 mmol) were added. The reaction mixture was stirred at 80 °C for 20 h. Then, it was diluted by dichloromethane and washed by water. Organic phases were collected, dried ($MgSO_4$), and evaporated under reduced pressure. The residue was purified by flash chromatography on silica gel (gradient of diethyl ether in toluene/hexane (75/25 v/v)) and precipitated by pentane from THF to yield title product (15%, 9 mg) as a colorless solid glass: IR: 1641 (small intensity), 1590, 1142, 1040 cm^{-1}; ^1H NMR (600 MHz, $CDCl_3$, 25 °C) δ=7.63 (d, J=8.8 Hz, 2H), 7.19–7.37 (m, 240H), 6.88 (d, J=8.8 Hz, 2H), 6.80 (m, 2H), 6.70 (br s, 2H), 6.54–6.66 (m, 78H), 6.43–6.54 (m, 53H), 6.33 (d, J=8.8 Hz, 1H), 4.77–4.98 (m, 186H) ppm; ^{13}C NMR (200 MHz, $CDCl_3$, 25 °C) δ=160.13, 160.11, 160.09, 160.07, 160.05, 160.02, 160.00, 159.94, 139.24, 139.19, 139.17, 136.76, 136.74, 136.73, 128.53, 128.51, 128.50, 127.94, 127.91, 127.89, 127.51, 106.39, 106.35, 106.33, 101.56, 101.54, 101.53, 101.49, 101.47, 70.02, 70.00, 69.96, 69.91, 69.89, 69.88, 69.84 ppm. MS (MALDI-TOF) m/z found 10.121 $[M+H]^+$ calcd 10.092.

4.3. Spectroscopic measurements

UV/vis absorption and photoluminescence measurements were carried out on an absorption spectrometer (Shimadzu UV-2401-PC) and a fluorescence spectrophotometer (FLUOROMAX-P, Jobin Yvon), respectively, at ambient conditions, using standard 10 mm cells and THF as solvent.

Fluorescence quantum yields of each compound (Φ_x) were determined by the method described by Williams et al.,[35] using quinine sulfate (in 0.1 M H_2SO_4) as standard, which has a known fluorescence quantum yield (Φ_{ST}=0.54), according to

$$\phi_X = \phi_{ST}\frac{Grad_X}{Grad_{ST}}\frac{\eta_X^2}{\eta_{ST}^2}$$

where *Grad* is the slope from the plot of integrated fluorescence intensity versus absorbance at the same excitation wavelength, and η stands for the refractive index of the solvent (1.3332 for sulfuric acid solution of quinine, and 1.407 for THF).

Absorbances of five concentrations of the standard (in H_2SO_4) and each sample (in THF) were measured. Concentrations have been chosen, which provide absorbances lower that 0.1 at and above the excitation wavelength, to avoid inner filter effects.

Wavelength at which the standard and samples absorb (either 315 nm or 280 nm) was chosen as excitation wavelength. Emission spectra were recorded on the same solutions under constant conditions, 48 h after stabilization (slit width: 10 nm).

ORIGIN 8.0 was used for integrating the area of emission spectra. Residual fluorescence of solvents has been corrected. Five-point Area-Absorbance regressions were plotted for the standard and each compound.

Time-domain excited-state lifetimes were measured using an IBH 5000F coaxial nanosecond flashlamp, in a FL3-11 Fluorolog equipment.

Acknowledgements

Financial support by the Spanish Ministry of Economy and Competitiveness, with the participation of European Union (MINECO, projects CTQ2010-16959/BQU, CTQ2012-35535 and Consolider-Ingenio CSD2007-00006), from the University of the Basque Country (UPV/EHU, UFI11/22 QOSYC), from the Basque Government (GV/EJ, grant IT-324-07), from the Donostia International Physics Center (DIPC), from the Ministry of Education, Youth and Sports of the Czech Republic (grant MSM6046137305), and Czech Science Foundation (projects 304/10/1951, P503/11/0616) is acknowledged. M.d.B. thanks the CSIC for the JAE-Pre contract funding for her PhD. The authors also thank the SGI/IZO-SGIker UPV/EHU and the DIPC for generous allocation of computational resources.

Supplementary data

Scanned photocopies of ^{1}H and ^{13}C NMR data and MD input files (*Maestro-Macro Model* format) were supported. Supplementary data related to this article can be found at http://dx.doi.org/10.1016/j.tet.2013.10.002.

References and notes

1. Buhleier, G. E.; Wehner, W.; Vögtle, F. *Synthesis* **1978**, 155.
2. Tomalia, D. A.; Naylor, A. M.; Goddardt, W. A., III. *Angew. Chem., Int. Ed. Engl.* **1990**, *29*, 138; *Angew. Chem.* **1990**, *102*, 119.
3. (a) Newcome, G. P.; Moorefield, C. N.; Vögtle, F. *Dendritic Molecules: Concepts, Synthesis, Perspectives*; Wiley-VCH: Weinheim, Germany, 1996; (b) Newcome, F. G. R.; Moorefieeld, C.; Vögtle, F. *Dendrimers and Dendrons*; Wiley-VCH: Weinheim, Germany, 2001; (c) Vögtle, F.; Richardt, G.; Werner, N. *Dendrimer Chemistry—Concepts, Synthesis, Properties, Applications*; Wiley-VCH: New York, NY, 2009.
4. (a) Majoral, J.-P.; Caminade, A.-M. *Chem. Rev.* **1999**, *99*, 845; (b) Grayson, S. M.; Fréchet, J. M. J. *Chem. Rev.* **2001**, *101*, 3819; (c) Bronstein, L. M.; Shifrina, Z. B. *Chem. Rev.* **2011**, *111*, 5301; (d) Newkome, G. R.; Schreiner, C. *Chem. Rev.* **2010**, *110*, 6338; (e) Walter, M. V.; Malkoch, M. *Chem. Soc. Rev.* **2012**, *41*, 4593; (f) Astruc, D.; Liang, L.; Rapakousiou, A.; Ruiz, J. *Acc. Chem. Res.* **2012**, *45*, 630.
5. (a) Astruc, D.; Chardac, F. *Chem. Rev.* **2001**, *101*, 2991; (b) Heerbeek, R. v.; Kamer, P. C. J.; Leeuwen, P. W. N. M. v.; Reek, J. N. H. *Chem. Rev.* **2002**, *102*, 3717; (c) Caminade, A.-M.; Ouali, A.; Keller, M.; Majoral, J.-P. *Chem. Soc. Rev.* **2012**, *41*, 4113.
6. (a) Lo, S.-C.; Burn, P. L. *Chem. Rev.* **2007**, *107*, 1097; (b) Astruc, D.; Boisselier, E.; Ornelas, C. *Chem. Rev.* **2010**, *110*, 1857.
7. Zeng, F.; Zimmermann, S. Z. *Chem. Rev.* **1997**, *97*, 1681.
8. (a) Stiriba, S.-E.; Frey, H. F.; Haag, R. *Angew. Chem., Int. Ed.* **2002**, *41*, 1329 *Angew. Chem.* **2002**, *114*, 1385; (b) Tekade, R. K.; Kumar, P. V.; Jain, N. K. *Chem. Rev.* **2009**, *109*, 49; (c) Medina, S. H.; El-Sayed, M. E. H. *Chem. Rev.* **2009**, *109*, 3141; (d) Vilaraza, A. J. L.; Bumb, A.; Brechbiel, M. W. *Chem. Rev.* **2010**, *110*, 2921; (e) Mintzer, M. A.; Grinstaff, M. W. *Chem. Soc. Rev.* **2011**, *40*, 173; (f) Gajbhiye, V.; Palanirajan, V. K.; Tekade, R. K.; Jain, N. K. *J. Pharm. Pharmacol.* **2009**, *61*, 989.
9. (a) Biricova, V.; Laznickova, A. *Bioorg. Chem.* **2009**, *37*, 185; (b) Caminade, A.-M.; Laurent, R.; Majoral, J.-P. *Adv. Drug Delivery Rev.* **2005**, *57*, 2130.
10. Ballauff, M.; Likos, C. N. *Angew. Chem., Int. Ed.* **2004**, *43*, 2998; *Angew. Chem.* **2004**, *116*, 3060.
11. De Gennes, P. G.; Hervet, H. *J. Phys., Lett.* **1983**, *44*, 1351.
12. Lescanec, R. L.; Muthukumar, M. *Macromolecules* **1990**, *23*, 2280.
13. (a) Caminade, A.-M.; Hameau, A.; Majoral, J.-P. *Chem.—Eur. J* **2009**, *15*, 9270; (b) Jian, W.; Ju, M.; AnJun, A.; JingZhi, S.; Zhong, T. B. *Sci. China Chem.* **2010**, *53*, 2409.
14. (a) Grabchev, I.; Staneva, D.; Betcheva, R. *Curr. Med. Chem.* **2012**, *19*, 4976; (b) Albertazzi, L.; Brondi, M.; Pavan, G. M.; Sato, S. S.; Signore, G.; Storti, B.; Ratto, G. M.; Beltram, F. *Plos One* **2011**, *6*, e28450; (c) Pugh, V. J.; Hu, Q.-S.; Pu, L. *Angew. Chem., Int. Ed.* **2000**, *39*, 3638 *Angew. Chem.* **2000**, *112*, 3784.
15. Adronov, A.; Fréchet, J. M. J. *Chem. Commun.* **2000**, 1701.
16. Hwang, S. H.; Moorefield, C. N.; Newkome, G. R. *Chem. Soc. Rev.* **2008**, *37*, 2543.
17. Burn, P. L.; Lo, S. C.; Samuel, I. D. W. *Adv. Mater.* **2007**, *19*, 1675.
18. (a) Zubia, A.; Cossío, F. P.; Morao, I.; Rieumont, M.; Lopez, X. *J. Am. Chem. Soc.* **2004**, *126*, 5243; (b) Morao, I.; Cossío, F. P. *Tetrahedron Lett.* **1997**, *38*, 6461.
19. Xiao, M.; Yan, W.; Zhang, Z. *J. Chem. Eng. Data* **2010**, *55*, 3346.
20. (a) Bowen, J. P.; Allinger, N. L. In *Reviews in Computational Chemistry*; Lipkowitz, K. B., Boyd, E. D., Eds.; VCH: New York, NY, 1991; Vol. 2, pp 81–97; (b) Allinger, N. L.; Yuh, Y. H.; Lii, J.-H. *J. Am. Chem. Soc.* **1989**, *111*, 8551; (c) Lii, J.-H.; Allinger, N. L. *J. Am. Chem. Soc.* **1989**, *111*, 8576.
21. Theodorov, D. N.; Suter, U. W. *Macromolecules* **1985**, *18*, 1206.
22. Kinoshita, M. *Chem. Phys. Lett.* **2004**, *387*, 54.
23. (a) Toptygin, D. *J. Fluoresc.* **2003**, *13*, 201; (b) Toptygin, D.; Savtchenko, R.; Meadow, N. D.; Roseman, S.; Brand., L. *J. Phys. Chem.* **2002**, *106*, 3724.
24. Amat, A.; Clementi, C.; De Angelis, F.; Sgamellotti, A.; Fantacci., S. *J. Phys. Chem. A* **2009**, *113*, 15118.
25. Favaro, G.; Clementi, C.; Romani, A.; Vickackaite, V. *J. Fluoresc.* **2007**, *17*, 707.
26. Allinger, N. L. *Molecular Structure. Understanding Steric and Electronic Effects from Molecular Mechanics*; Wiley: Hoboken, NJ, 2010.
27. (a) Haile, J. *Molecular Dynamics Simulations*; Wiley: New York, NY, 1992; (b) Cramer, C. J. *Essentials of Computational Chemistry*; Wiley: Chichester, UK, 2002; pp 63–94; and references therein.
28. (a) MacroModel, Version 9.9; Schrodinger LLC: New York, NY, 2012; (b) Mohamadi, F.; Richards, N. G. J.; Guida, W. C.; Liskamp, R.; Lipton, M.; Caulfield, C.; Chang, G.; Hendrickson, T.; Still, W. C. *J. Comput. Chem.* **1990**, *11*, 440.
29. Rickaert, J. P.; Ciccotti, G.; Berendsen, H. J. C. *J. Comput. Phys.* **1977**, *23*, 327.
30. (a) Naidoo, K. J.; Hughes, S. J.; Moss, J. R. *Macromolecules* **1999**, *32*, 331; (b) Teobaldi, G.; Zerbetto, F. *J. Am. Chem. Soc.* **2003**, *125*, 7388; (c) Karatajos, K.; Adolf, D. B.; Davies, G. R. *J. Chem. Phys.* **2001**, *115*, 5310; (d) Lee, I.; Athey, B. D.; Wetzel, A. W.; Meixner, W.; Baker, J. R., Jr. *Macromolecules* **2002**, *35*, 4510.
31. Field, M. J. *A Practical Introduction to the Simulation of Molecular Systems*; Cambridge University Press: Cambridge, UK, 1999.
32. (a) Hawker, C. J.; Fréchet, J. M. J. *J. Am. Chem. Soc.* **1990**, *112*, 7638; (b) Hawker, C. J.; Fréchet, J. M. J. *J. Chem. Soc., Chem. Commun.* **1990**, 1010.
33. Machida, K.; Osawa, K. *Chem. Pharm. Bull.* **1989**, *37*, 1092.
34. Shan, M. D.; O'Doherty, G. A. *Org. Lett.* **2006**, *8*, 5149.
35. Williams, A. T. R.; Winfield, S. A.; Miller., J. N. *Analyst* **1983**, *108*, 1067.